ChemistrySelect

Research Article
doi.org/10.1002/slct.202200355

Chemistry Europe
European Chemical Societies Publishing

www.chemistryselect.org

Catalysis

Magnetic Nanoparticles Supported on g-C_3N_4 : An Efficient Heterogeneous Catalyst for Selective Transfer Hydrogenation of Furfural to Furfuryl alcohol

Purashri Basyach[a, b] and Lakshi Saikia*[a, b]

A series of economic and environmental benign g-C_3N_4 supported magnetic ferrite nanoparticles (Fe_3O_4@g-C_3N_4) were synthesized for the catalytic transfer hydrogenation of furfural (FF) into furfuryl alcohol (FFA) using ethanol as a source of hydrogen donor and solvent. The unique feature of high nitrogen content and locally conjugated structure of the g-C_3N_4 have made it excellent support for loading of small sized ferrite nanoparticles. Excellent furfural conversion of 95.6% was obtained with 100% selectivity of the required product furfuryl alcohol over this Fe_3O_4@g-C_3N_4 nanoparticles having mass ratio 0.2 of Fe_3O_4@g-C_3N_4. The high surface properties, uniform dispersion of ferrite and very high ability of adsorption of furfural over g-C_3N_4 attributed to the effective catalytic activity. The effect of iron content, catalyst amount, solvent, temperature and reaction time on the CTH of furfural were studied. The synthesized catalysts were characterised by various physic-chemical, spectroscopic and microscopic techniques.

Introduction

The production of fuels and value-added chemicals also known as 'biorefinery' has attracted much attention considering the catastrophe of fossil resources and the growing environmental concerns.[1,2] Conversion of lignocellulosic biomass into fuels and chemicals currently becomes a very promising and challenging issue in the field of catalyst design as they are abundantly available and can be used as fossil resources to supply chemicals and fuels.[3,4] Again, Furfural, being a compound having highly functionalised groups such as C–O, C=C and C=O can act as essential platform compound in the development of lignocellulose based various biofuels and valuable chemicals through reactions like hydrogenation, oxidation, aldol condensation etc.[5,6] Catalytic hydrogenation of C5 carbohydrates takes prominent role in the production of furfural which can be transformed into variety of compounds through many reactions.[7] Especially, hydrogenation of furfural has gained massive importance as many industrially applicable chemicals and biofuels such as furfuryl alcohol, tetrahydrofurfuryl alcohol, 2-Methylfuran etc. are obtained from it.[8–10]

Furfuryl alcohol acts as an important intermediate in the manufacture of many chemicals such as vitamin C, lysine, resins, lubricants, plasticizer etc.[11,12] The hydrogenation of furfural (FF) to furfuryl alcohol (FFA) can be accomplished industrially in a liquid or vapour phase.[13] In the gas phase hydrogenation (i.e. under high H_2 pressure) of FF to FFA, copper-based catalyst is used for high selectivity. But, the main flaw of this method is the expenditure of large amount of energy needed for the vapourisation of FF.[14,15] In this fashion, liquid phase hydrogenation is considered as more desirable in industrial process and the process involves copper chromate as catalyst for the high selective hydrogenation of FF to FFA.[18] But Cr_2O_3 is highly toxic and the use of this catalyst may cause drastic environmental pollution.[13,16] Therefore, a lots of chromium-free catalysts are synthesised to accomplish an environmentally favourable hydrogenation of FF to FFA. However, non-noble metal catalysed conventional liquid-phase hydrogenation continues to demand elevated hydrogen pressure thus making this process more costly.[19,20] Nonetheless, considerable attempts have recently been made for the generation of "green hydrogen" through water splitting or biomass gasification yet most of the industrially produced hydrogen is obtained from inextensible fossil resources.[6,21,22]

In the light of these facts, catalytic transfer hydrogenation (CTH) of furfural has recently encountered as a substitutional excess for the reduction of biomass derived molecules.[23] This process sounds like more cost effective and safer as it avoids the use of explosive hydrogen. Different alcohols such as primary or secondary alcohols or organic acids can be used as hydrogen donor in catalytic transfer hydrogenation reaction. This transfer hydrogenation process with alcohols is mainly based on Meerwein-Ponndorf-Verley (MPV) reduction, in which carbonyl compounds are selectivity reduced to the corresponding hydroxyl compounds.[24] The ambigious role of the alcohol as solvent and H-donor along with the bounteous, economical and easily storable characteristics of alcohols, has facilitated the utilization of CTH with biomass-derived molecules.[25,26] The CTH

[a] P. Basyach, Dr. L. Saikia
Materials Science & Technology Division,
CSIR-North East Institute of Science and Technology,
Jorhat-785006, Assam, India
E-mail: lsaikia@neist.res.in
l.saikia@gmail.com
[b] P. Basyach, Dr. L. Saikia
Academy of Scientific and Innovative Research (AcSIR),
Ghaziabad-201002, UP, India

Supporting information for this article is available on the WWW under https://doi.org/10.1002/slct.202200355

of FF has been extensively studied over many catalytic systems like supported and/or unsupported metals (e.g.; Pd/C,[27] Cu–Pd/C,[28] Cu–Ni[29]), metal oxides (e.g.; $Ru/RuO_2/C$[30]) etc. In addition to the metal catalysts, some reports on Lewis acidic zeolites (e.g.; Ti(IV), Sn(IV), and Zr(IV)) were also found to boost the CTH of furfural into furfural alcohol.[31,32] The development of an advanced catalytic pathway for proficient CTH of furfural into furfuryl alcohol is still enviable.

Now-a-days magnetic catalysts have achieved more attention in the catalytic world due to easily recoverable quality of magnetic catalysts from a reaction mixture by using an external magnet. Thus, it can avoid the loss of more amounts of catalysts during recyclization. As iron salts are cost effective, non -toxic and easily available magnetic ferrite nanoparticles are more demanding in the field of catalysis like organic synthesis.[33,34] He et al. performed a comparative study of the catalytic activity of Fe_3O_4, $CoFe_2O_4$ and $NiFe_2O_4$ in catalytic transfer hydrogenation reaction, and observed that amongst them $NiFe_2O_4$ showed the highest catalytic activity in terms of conversion and selectivity.[35] Recently, Fan Van et al. reported the CTH of FF to FFA of 91.7% selectivity by using magnetic γ-Fe_2O_3@HAP using IPA as hydrogen donor.[16] Jiang Li et al. reported that by using N-doped carbon supported iron catalysts 91.6% conversion of FF to FFA can be done with 83% selectivity.[13]

2D graphitic carbon nitride (g-C_3N_4) has become the most promising nanocatalyst amongst various supporting material explored. As graphite like structure, g-C_3N_4 is the most stable allotrope of carbon nitride at ambient atmosphere.[36] g-C_3N_4 nanocatalysts can be easily prepared by the thermal polymerisation of urea, thiourea, melamine, cyanamide etc. The high nitrogen content makes its surface properties more valuable for catalysis, such as basic surface functionalities, electron rich properties, H-motifs etc. Additionally, its high thermal stability (upto 600 °C in air) empowers the material to be active either in liquid or gaseous environment. The high surface properties make its dispersion excellent and this enables g-C_3N_4 with anchoring small sized metal or metal oxide nanoparticles. The magnetic ferrite nanoparticles can also be easily immobilised over g-C_3N_4 which makes them highly active in some catalytic reduction reaction such as hydrogenation reaction. Baig et al. recently reported the photocatalytic hydrogenation of alkene or alkynes using magnetic Fe_3O_4@g-C_3N_4.[37] Because of the intrinsic 2D layer structure of g-C_3N_4, it has high electron mobility and also provides more reactive sites for adsorption of substrate molecules which also helps in transfer of hydrogen in catalytic transfer hydrogenation reaction.

In the present work, g-C_3N_4 supported magnetic ferrite nanoparticles (Fe_3O_4@g-C_3N_4) have been illustrated for transfer hydrogenation of FF to FFA using green solvent ethanol as hydrogen donor and also as solvent. This application has demonstrated that magnetic Fe_3O_4@g-C_3N_4 can act as useful and superior catalyst in highly selective production of furfuryl alcohol.

Results and Discussion

Catalyst characterisation

The desired nanocomposite was synthesised in a two-step process. At first, g-C_3N_4 was synthesised via thermal polymerisation and secondly g-C_3N_4 supported magnetic ferrite nanoparticles (Fe_3O_4@g-C_3N_4) were synthesised via ultrasound mediated reduction method using $NaBH_4$ as a reducing agent. A schematic diagram of the synthesis method is illustrated in Figure 1. The as synthesised catalysts were characterised by different techniques.

The XRD patterns of as prepared g-C_3N_4 and magnetic Fe_3O_4@g-C_3N_4 are presented in Figure 2a and 2b. It is observed that all the samples contain two distinct diffraction peaks of graphitic carbon nitride. The most potent peak at 27.4° corresponding to (002) crystal plane of graphitic materials represents the characteristic interlayer stacking structure of conjugated aromatic system of triazine ring. The interplaner

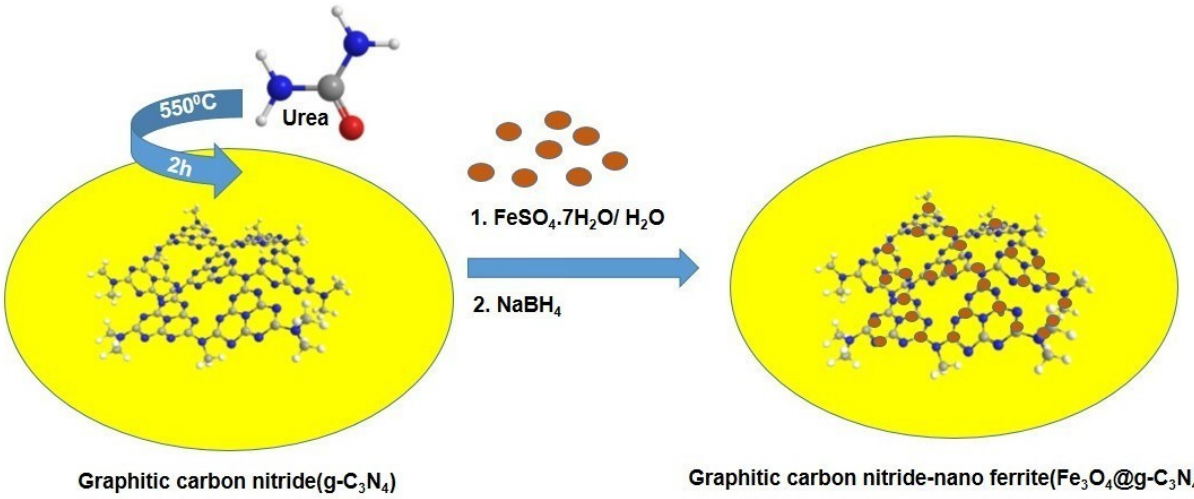

Figure 1. Synthesis of magnetic Fe_3O_4@g-C_3N_4.

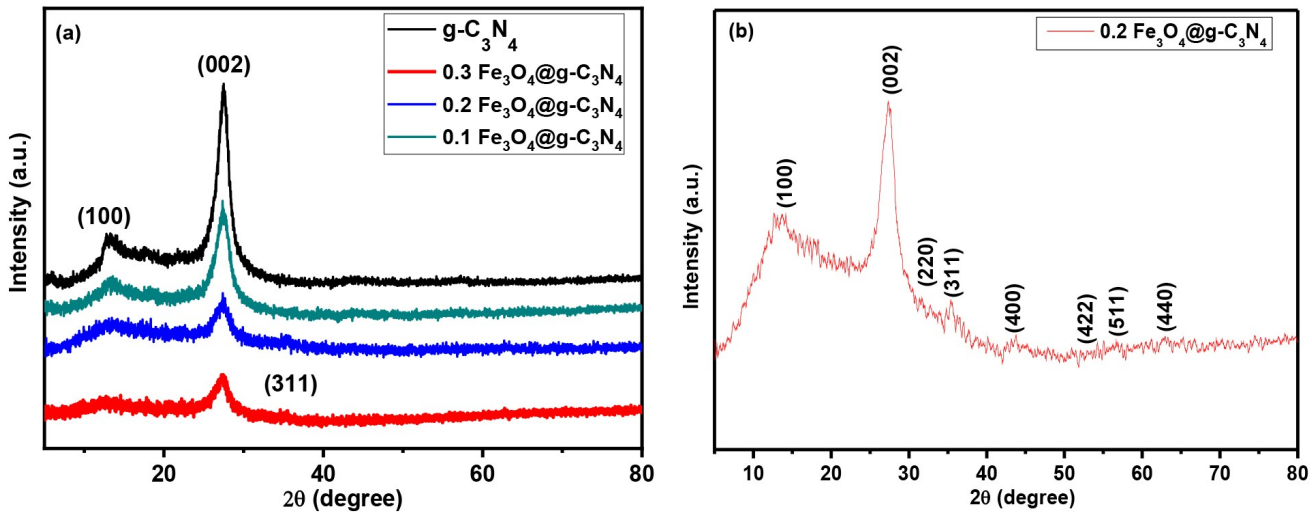

Figure 2. (a) PXRD pattern of as synthesized catalysts and (b) PXRD pattern of 0.2 Fe_3O_4@g-C_3N_4.

distance is found to be 0.322 nm which is almost similar to the reported results.[38] The small peak at 13.2° reflecting the (100) plane of g-C_3N_4 is connected with interlayer staking with an interplaner distance of 0.686 nm.[39] After the impregnation of the magnetic nanoparticles the intensity of the above two peaks in XRD pattern was decreased signifying the close intact between Fe species and g-C_3N_4.[40] But with the increase of the mass ratio of Fe and g-C_3N_4, peaks of magnetic ferrites (Fe_3O_4) show up at about 30.1°, 35.4°, 43.2°, 54.1°, 56.9°, 62.8° corresponding to planes (220), (311), (400), (422), (511), (440) respectively (Figure 2b).

Figure 3 depicts the FTIR spectra of g-C_3N_4 and 0.2 Fe_3O_4@g-C_3N_4. The strong bands between 1230 and 1647 cm^{-1} are associated with the characteristic stretching vibration mode of carbon nitride heterocycles.[41] The FT-IR band at 809 cm^{-1} corresponds to the triazine unit implying the existence of conventional structure of g-C_3N_4.[42] The wide bands at 3020–3600 cm^{-1} indicate the presence of NH or NH_2 groups.[40] The FT-IR spectrum of 0.2 Fe_3O_4@g-C_3N_4 is almost identical to that of the g-C_3N_4, except that another small band is at 584.1 cm^{-1} signifying the existence of Fe–O bond in the compound.

The N_2 adsorption-desorption isotherms of pure g-C_3N_4 and 0.2 Fe_3O_4@g-C_3N_4 catalysts are depicted in the Figure 4. The Brunauer-Emmet-Teller (BET) surface area and pore volume of pure g-C_3N_4 were found to be 48 $m^2 g^{-1}$ and 0.17 $cm^3 g^{-1}$ respectively. While the 0.2 Fe_3O_4@g-C_3N_4 exhibited a BET

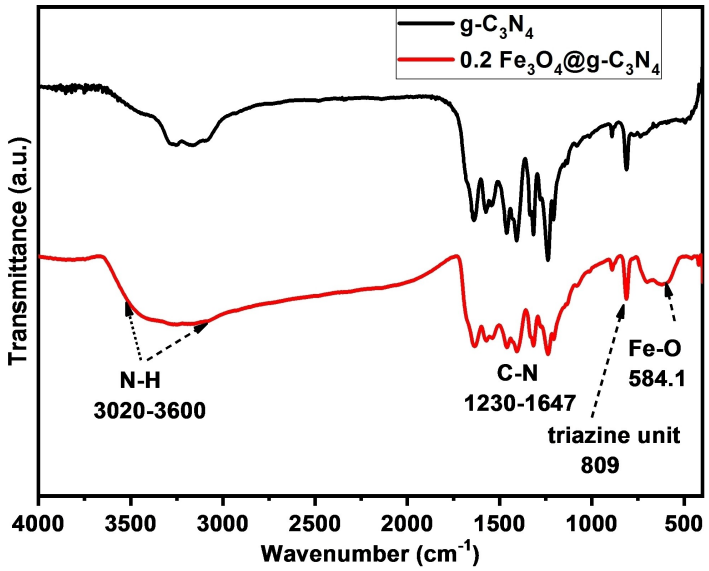

Figure 3. FTIR spectra of g-C_3N_4 and 0.2 Fe_3O_4@g-C_3N_4.

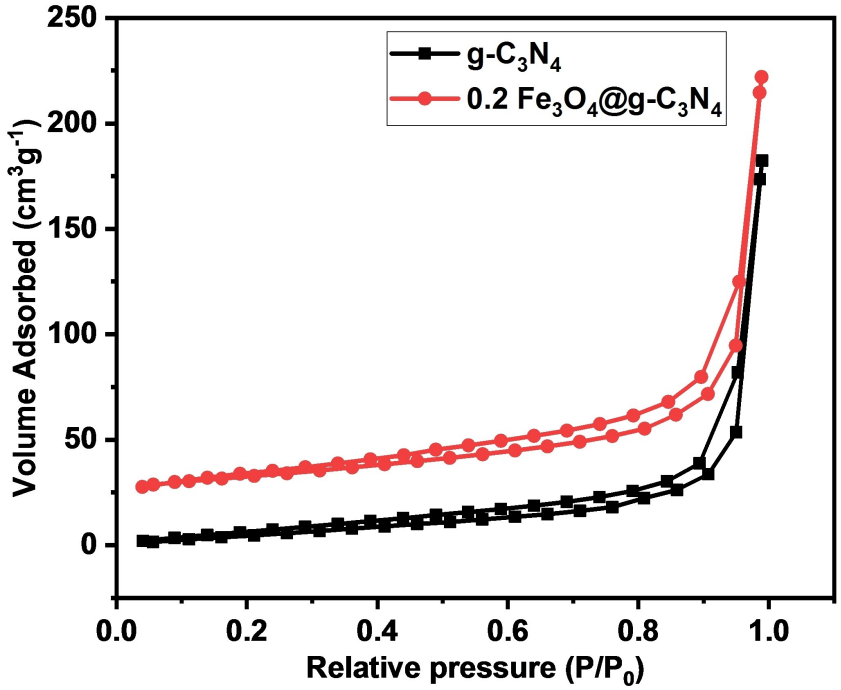

Figure 4. Nitrogen adsorption-desorption isotherms of the as prepared samples.

surface area of 52.2 m^2g^{-1} with pore volume 0.31 cm^3g^{-1}. The increase in surface area of Fe_3O_4@g-C_3N_4 with the incorporation of iron species over g-C_3N_4 catalyst may be because of the creation of new pores, modification of surface of carbon nitride pore structure and effective diffusion of magnetic ferrite nanoparticles into g-C_3N_4 support during the pre-treatment of g-C_3N_4 support and time of reduction with $NaBH_4$ which causes increase in surface roughness without blocking pores.[43]

For further investigation of the chemical states of the elements present in the nanocomposite, XPS analysis was performed (Figure 5). The XPS survey spectrum clearly shows the presence of elements C, N, O, Fe on the catalytic surface of Fe_3O_4@g-C_3N_4 at binding energies of 286.9 eV (C1s), 397.9 eV (N1s), 529.9 eV (O1s) and 710.2 eV (Fe2p) having concentration of 41.49%, 48.47%, 7.72% and 2.32%, respectively (Figure 5a). In the high resolution spectra of C1s (Figure 5b) two deconvoluted peaks are observed at binding energies of 283.7 eV and 286.8 eV, assigning to graphitic carbon (C–C) and sp^2-bonded carbon (N–C=N) respectively.[44] Figure 5c depicts the high resolution N1s spectra for 0.2 Fe_3O_4@g-C_3N_4, where N1s is deconvoluted into three states such as triazine rings, C=N–C (397.2 eV), tertiary nitrogen, N-$(C)_3$ (398.8 eV) and the amino functions, N–H (402.6 eV) indicating the presence of heptazine ring of g-C_3N_4 in the compound Fe_3O_4@g-C_3N_4.[45] As depicted in Figure 5d, two main peaks of O1s are observed with binding energies of 528.8 eV and 531.4 eV correspond to the lattice oxygen of the magnetic ferrites and the –OH of water molecules.[46] The high resolution Fe2p XPS spectra are shown in the Figure 5e. The two main peaks of Fe2p corresponding to the $Fe2p_{3/2}$ and $Fe2p_{1/2}$ can be deconvoluted into six peaks at 709.7, 712.8, 717.8, 723.7, 725.9 and 732.9 eV. The four peaks corresponding to Fe^{2+} (709.7 eV and 723.7 eV) and Fe^{3+} (712.8 eV and 725.9 eV) states confirm the presence of Fe_3O_4 phase in the composite. Again, the small peaks at around 717.8 eV and 732.9 eV attribute to the satellite peaks of Fe^{3+} of Fe_2O_3 phase, indicating the presence of very small amount of γ-Fe_2O_3.[47,48]

For morphological studies SEM, TEM and HRTEM analysis of pure g-C_3N_4 and 0.2 Fe_3O_4@g-C_3N_4 were also performed. Figure 6a depicts the SEM image of closed stacking arrangement of conjugated aromatic system of pure g-C_3N_4 with several smaller disordered particles over the surface. This can be attributed to the mild rupture of layers during the crystal growth.[49] Figure 6b displays the SEM image of material 0.2 Fe_3O_4@g-C_3N_4, where a considerable amount of uneven smaller particles are observed due to the aggregation of ferrite nanoparticles over g-C_3N_4 support.[50]

The elemental composition of the both compounds are obtained from the EDX pattern of g-C_3N_4 and 0.2 Fe_3O_4@g-C_3N_4 indicating the presence of C, N, Fe & O in the compounds (Figure 6c). The TEM image of g-C_3N_4 (Figure 6d) depicts the sheet like structure of g-C_3N_4 with diameters of few nanometres. In the magnified TEM image (Figure 6e) of composite 0.2 Fe_3O_4@g-C_3N_4, homogeneous distributions of ferrite nano-

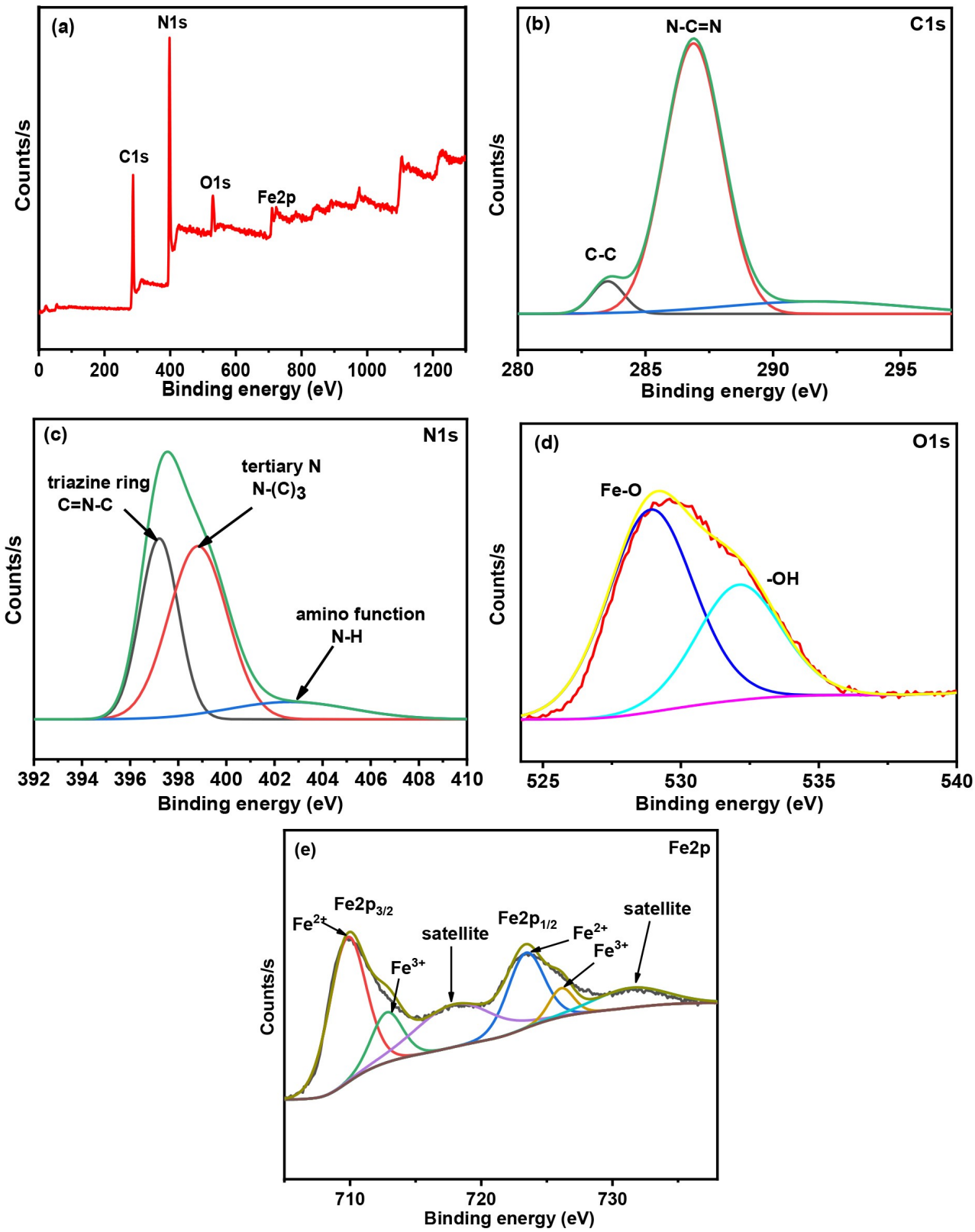

Figure 5. (a) XPS survey, (b) C1s XPS spectra, (c) N1s XPS spectra, (d) O1s XPS spectra, (e) Fe2p XPS spectra of 0.2 Fe_3O_4@g-C_3N_4 catalyst.

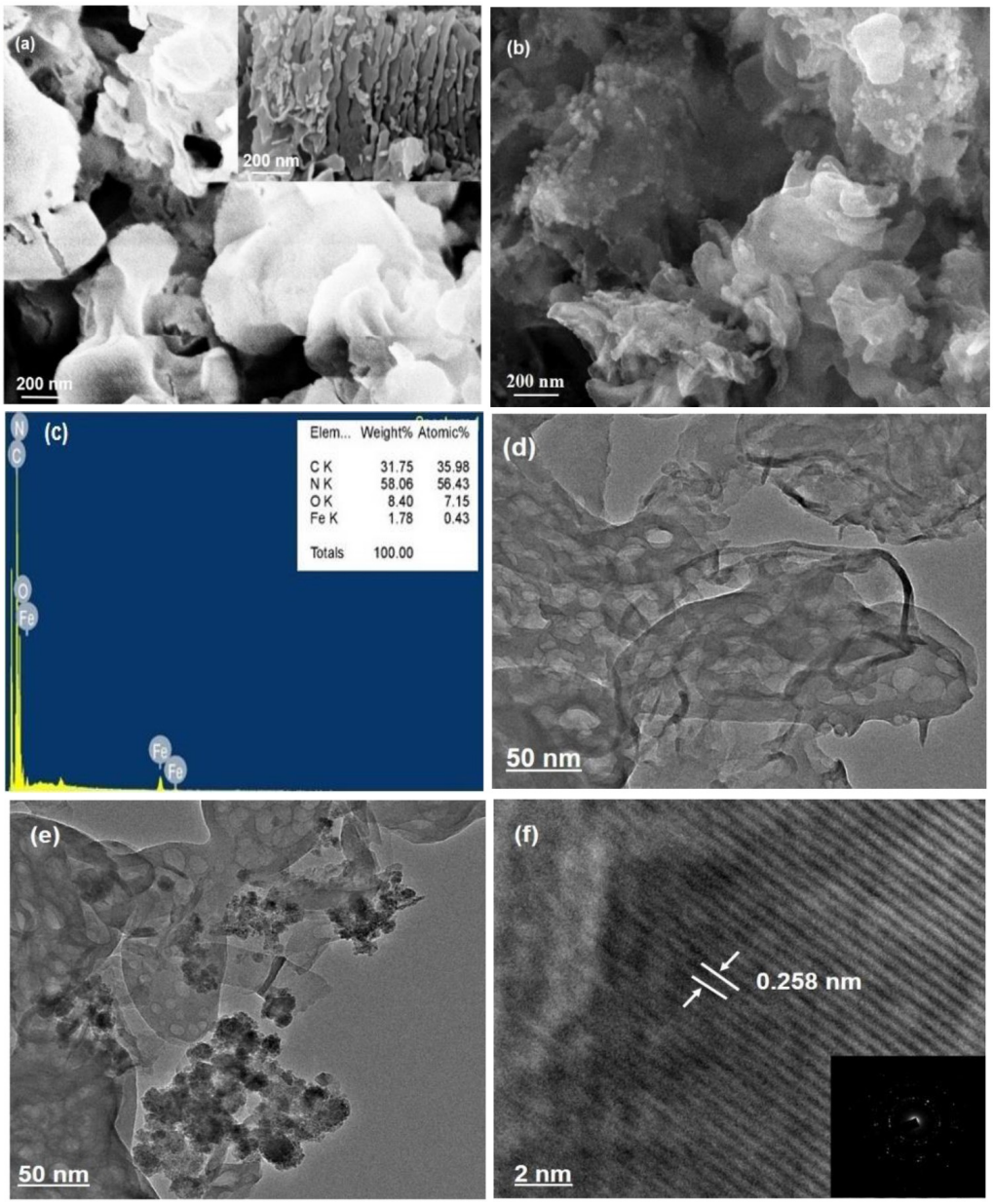

Figure 6. (a) FESEM image of prepared g-C_3N_4 catalyst, (b) FESEM image of 0.2 Fe_3O_4@g-C_3N_4 catalyst, (c) EDX of as synthesized 0.2 Fe_3O_4@g-C_3N_4 catalyst, (d) TEM image of support g-C_3N_4, (e) TEM image of 0.2 Fe_3O_4@g-C_3N_4 catalyst, (f) HRTEM image of 0.2 Fe_3O_4@g-C_3N_4 catalyst along with the SAED pattern.

particles having spherical morphology is seen over the surface of g-C_3N_4. From the TEM image indexed in Figure 6e, the diameter of majority of the ferrite nanoparticles is observed to be less than 5 nm and size of some particles is found to be greater than 5 nm. So, the average diameter of the ferrite particles can be considered to be around 5 nm. The HRTEM image of 0.2 Fe_3O_4@g-C_3N_4 is shown in Figure 6f. The average interlayer spacing (d) is calculated as 0.25 nm which confirms the presence of (311) plane of magnetic ferrites over the surface of g-C_3N_4. The formation of crystalline phases over the support can be distinguished from the diffused rings present in the selected area electron diffraction (SAED) pattern (Figure 6f), which appears as a consequence of the interaction of the ferrite nanoparticles with the g-C_3N_4 support.[51]

Catalytic transfer hydrogenation (CTH) of furfural into furfuryl alcohol

Catalyst screening for CTH of furfural into furfuryl alcohol

Effect of iron loading

The as prepared g-C_3N_4 supported magnetic ferrite nanoparticles were investigated for the transfer hydrogenation of furfural with ethanol as both the solvent and the hydrogen

donor. The effect of different parameters were also studied for the optimisation of the reaction. The reaction pathway is shown in Scheme 1.

The results of different catalysts employed for CTH reaction are summarised in Table 1.

The effect of iron loading is also studied for this CTH reaction. As expected without any catalyst, there is no conversion of furfural (FF) (Table 2, entry 1). With pure magnetic ferrites nanoparticles and with pure g-C_3N_4 very poor conversion and poor selectivity (entry 10, 11) are observed. When the transfer hydrogenation was performed with g-C_3N_4 supported magnetic ferrite nanoparticles an increase in the conversion of FF to FFA is observed and is confirmed by GC analysis. This can be attributed to the incorporation of small sized ferrite nanoparticles over the 2D g-C_3N_4 surface enhances its surface area to some extent resulting in increasing its active catalytic sites for transfer hydrogenation reaction. With 0.05 Fe_3O_4@g-C_3N_4 (mass ratio of Fe_3O_4/g-C_3N_4), 48.5% conversion of FF is detected. However, the selectivity of the target product is not satisfactory (entry 2). The low selectivity of the target product may be due to the formation of some other by-products such as acetaldehyde, 2-Furaldehyde diethyl acetal etc. The C=O bond present in furfural (FF) undergoes hydrogenation and saturation to produce furfuryl alcohol (FFA).[52]

Subsequent increase in the iron loading upto 0.2 mass ratio of Fe_3O_4@g-C_3N_4 results in almost 95.6% conversion of FF with 100% selectivity of required product FFA (entry 7). This can be ascribed to the decrease in the yield of by-product acetal (2-Furaldehyde diethyl acetal, (Figure S8, ESI) produced during the reaction which led to the high selectivity of FFA. Further increasing iron loading upto 0.30 a lowering of conversion of FF is observed. The selectivity is also noticed to be slightly dropped down to 92.7% (Table 2, entry 9) due to the formation of other products. It is also seen that with 2 mmol of furfural 86.8% conversion of FF is obtained with 82.5% selectivity of FFA (entry 12). Thus, it can be accomplished that all the g-C_3N_4 supported magnetic ferrites catalysts screened very interestingly. However, 0.2 Fe_3O_4@g-C_3N_4 catalyst is found to be the best catalyst for highly selective production (100%) of desired product FFA and this may be due to good dispersion of ferrite nanoparticles in g-C_3N_4 suspension and presence of appropriate

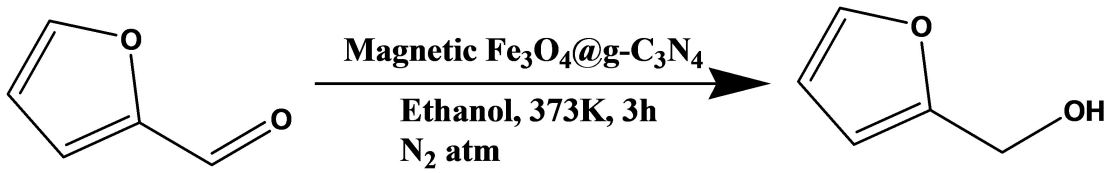

Scheme 1. Reaction pathway of transfer hydrogenation of furfural into furfuryl alcohol

Table 1. Catalytic transfer hydrogenation of furfural over various catalysts.[a]

Entry	Catalyst	Mass ratio (Fe_3O_4/g-C_3N_4)	% conversion of FF	% selectivity of FFA
1	Without catalyst	0	0	0
2	Fe_3O_4@g-C_3N_4	0.05	48.5	72.6
3	Fe_3O_4@g-C_3N_4	0.10	68.4	78.8
4	Fe_3O_4@g-C_3N_4	0.12	75.1	84.6
5	Fe_3O_4@g-C_3N_4	0.15	78.9	88.5
6	Fe_3O_4@g-C_3N_4	0.17	83.6	93.4
7	Fe_3O_4@g-C_3N_4	0.20	95.6	100
8	Fe_3O_4@g-C_3N_4	0.25	96.1	94.2
9	Fe_3O_4@g-C_3N_4	0.30	97.2	92.7
10	Magnetic ferrites	0	45.3	10.1
11	g-C_3N_4	–	≈5.1	–
12[b]	Fe_3O_4@g-C_3N_4	0.20	86.8	82.5

[a]Reaction conditions: Furfural (1 mmol), ethanol (10 ml), catalyst (20 mg), N_2 atmosphere, 373 K, 3 h, [b]reaction performed with 2 mmol of furfural under same reaction condition

Table 2. Effect of solvent in catalytic transfer hydrogenation of furfural.[a]

Entry	solvent	% conversion of FF	% selectivity of FFA
1	Isopropanol	97.1	80.4
2	Ethanol	95.6	100
3	Methanol	90.2	88.7
4	Secondary butyl alcohol	92.3	74.8
5	*t*-butyl alcohol	2.1	–

[a]Reaction conditions: Furfural (1 mmol), solvent (10 ml), catalyst (20 mg), N_2 atmosphere, 373 K, 3 h

amount of active catalytic sites which makes the catalyst more significant for selective transfer hydrogenation of FF.

Effect of catalyst amount in the CTH of Furfural

The effect of 0.2 Fe_3O_4@g-C_3N_4 catalyst amount in the CTH of furfural was surveyed and the results are depicted in Figure 7. As illustrated in Figure 7. it is noticeable to us that 84.8% conversion of furfural with 95.1% selectivity of FFA is observed with 10 mg of catalyst. The FF conversion increases gradually along with the catalyst amount. It is seen that with 20 mg of catalyst 95.6% conversion of furfural is detected with 100% selectivity of required product FFA. Further increasing the catalyst amount upto 100 mg, although the conversion of furfural increases, the selectivity of the product FFA is observed to be decreased to some extent. The presence of lots of catalytic sites in the high dosage of catalyst helps in the enhancement of conversion of FF, thereby accelerating the transfer hydrogenation. However, the low selectivity is attributed to generation of more by product acetal (2-Furaldehyde diethyl acetal) with the increase in the catalyst amount. Thus, it is fortified that highest selectivity of the required product FFA is observed with 20 mg of catalyst amount.

Effect of solvent

The selection of solvents usually has an impact on the catalytic activity of transfer hydrogenation. For this, certain general alcohols were used as hydrogen donor for the transfer hydrogenation of furfural over the 0.2 Fe_3O_4@g-C_3N_4 catalyst, and the observed results are summarised in Table 2.

Although the mechanism of the solvent effect on the heterogeneous catalyst is distinctly stated, it can be considered that catalytic activity is probably interconnected with the polarity and the structure of the solvent.[53] Among these solvents examined, it is found that primary alcohols, especially ethanol exhibits better performance, giving a 95.6% conversion of furfural with 100% selectivity of FFA (Table 2, entry 2). Methanol also shows a good result of 90.2% conversion of furfural with 88.7% selectivity of FFA (Table 2, entry 3). The slightly low selectivity of furfural in methanol than ethanol is due to the formation of more acetal product. Secondary alcohols like iso-propanol exhibits 97.1% conversion of furfural but with a poor selectivity 80.4% of FFA (Table 2, entry 1). The conversion of furfural is slightly lowered with other secondary alcohol like secondary butyl alcohol with a decrease in selectivity of FFA (Table 2, entry 4). In case of tertiary alcohol like *t*-butyl alcohol very less conversion of FF is observed. The reason should be that no hydrogen is present close to the hydroxyl group in *t*-butyl alcohol. The reason of better result of catalytic transfer hydrogenation in primary alcohols than secondary and tertiary alcohols like isopropanol, secondary butyl alcohol and *t*-butyl alcohol is due to high polarity of primary alcohols than the secondary alcohols and tertiary alcohols. The presence of bulky alkyl groups in isopropanol, secondary butyl alcohol and *t*-butyl alcohol may be the reason of low polarity of these alcohols which can hamper the transfer hydrogenation of furfural. The hydrogen donation capacity also depends on the reduction potential of lower alcohols used for the transfer hydrogenation reaction. It is known to us that the lesser the reduction potential the more is the reducing capacity. According to literature, reduction potential of lower alcohols is in the order: methanol > ethanol.[54] Although methanol is more polar than ethanol, the lower reduction potential of ethanol than that of methanol may be the reason of better conversion of FF and product selectivity than methanol in our work.

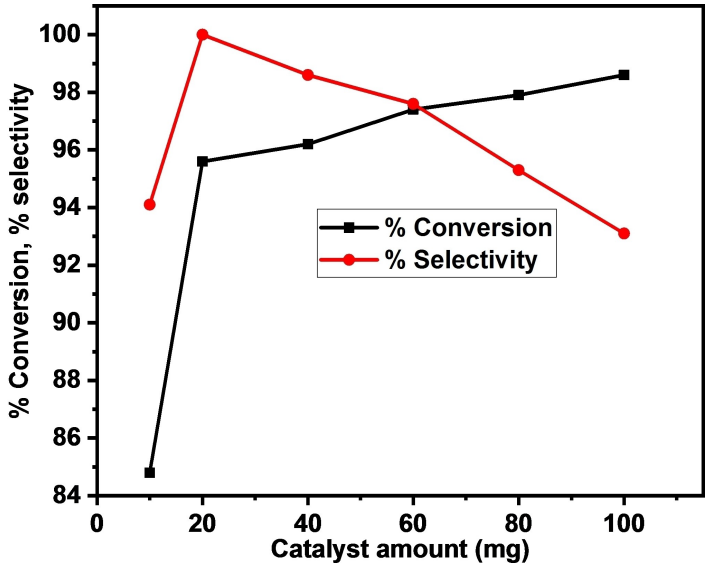

Figure 7. Effect of catalyst amount on the catalytic behaviour of 0.2 Fe_3O_4@g-C_3N_4 catalyst for the CTH of FF to FFA. Reaction conditions: 1 mmol FF, 10 mL ethanol, catalyst amount from 10 mg to 100 mg, 373 K, 3 h, N_2 atmosphere.

Effect of temperature

The temperature effect on the CTH of furfural into furfuryl alcohol over 0.2 Fe_3O_4@g-C_3N_4 was investigated comprehensively and the observed findings are presented in Figure 8. Predictably, temperature has a vital role in this CTH reaction. Around 85.4% conversion of FF with 89.7% selectivity of FFA are observed at 353 K for 3 h of reaction. But there is sudden increase in the conversion of FF upto 95.6% with 100% selectivity of furfural at 373 K temperature. This may be due to increase in reaction rate with increase in temperature. Further increasing the temperature from 393 K to 433 K, a gradual increase in conversion of FF is obtained with slight decrease in selectivity. The reason can be attributed to the excessive hydrogenation of the resulting FFA that supposed to be occurred at high temperature.

Effect of reaction time

Reaction time has considerable impact on CTH of FF to FFA which is summarised in Figure 9. A very low conversion of FF (18.4%) with 55.7% selectivity of FFA was obtained when the reaction was heated at 373 K for 30 minutes. After one hour, an increase in conversion of FF is observed with increasing selectivity. Further increase in reaction time from 90 minutes to 150 minutes, a gradual enhancement of conversion of FF is detected from 60.1% to 85.8% with high selectivity. The reaction reaches its optimum condition of 95.6% FF conversion with 100% selectivity of FFA at 373 K for 3 h of reaction, which is worth mentioning. The acceleration of the reaction with proceeding of reaction time may be because of the activation of Fe^{2+} and Fe^{3+} species present in the Fe_3O_4@g-C_3N_4. During the reaction course, the yield of side products acetal, acetaldehyde are also supposed to be decreased resulting in increase of the yield of the product FFA. However, further extending reaction time upto 4 hours the selectivity of the product FFA decreases to 96.8%. This can be explained on the basis of etherification of generated FFA during the reaction, which lowers the selectivity of FFA.

Kinetic study of CTH of furfural

To provide more insights into the catalytic transfer hydrogenation of FF to FFA over 0.2 Fe_3O_4@g-C_3N_4 catalyst, its kinetic studies were performed at four temperatures of 373 K, 393 K, 413 K and 433 K. In our reaction procedure ethanol was used in large excess; so, there was no effect of concentration of ethanol on the reaction kinetics. Thus, the transfer hydrogenation reaction could be proposed as a pseudo-first order reaction. As depicted in Figure 10a, reaction rate constant (k) was evaluated at each temperature from the corresponding slope of the plots of -ln(1-X) vs t (time), where x is the conversion of FF. The variation of rate constant k with temperature was presented in Figure 10b with the help of plot of lnk vs 1/T. The apparent activation energy E_a was determined from this slope of this Arrhenius plot. The E_a value was calculated to be 18 $kJmol^{-1}$ over the 0.2 Fe_3O_4@g-C_3N_4 for the CTH of FF into FFA with ethanol as the hydrogen donor. The activation energy value was found to be lower than many catalytic systems previously reported.[7,19]

Comparative study

A comparative study of the optimised catalyst 0.2 Fe_3O_4@g-C_3N_4 was surveyed with other previously reported catalysts for this transfer hydrogenation of furfural which is shown in the Table 3.

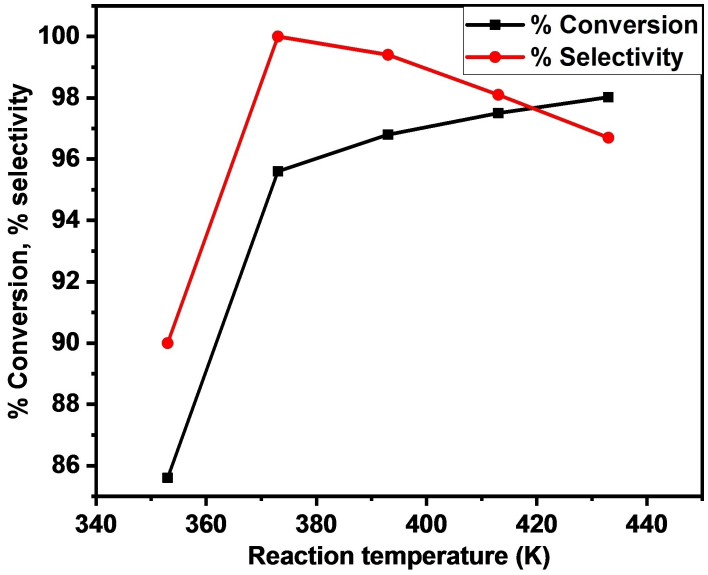

Figure 8. Effect of reaction temperature on the catalytic behaviour of 0.2 Fe_3O_4@g-C_3N_4 catalyst for the CTH of FF to FFA. Reaction conditions: 1 mmol FF, 10 mL ethanol, 20 mg catalyst, temperature from 353 K to 433 K, reaction time 3 h, N_2 atmosphere.

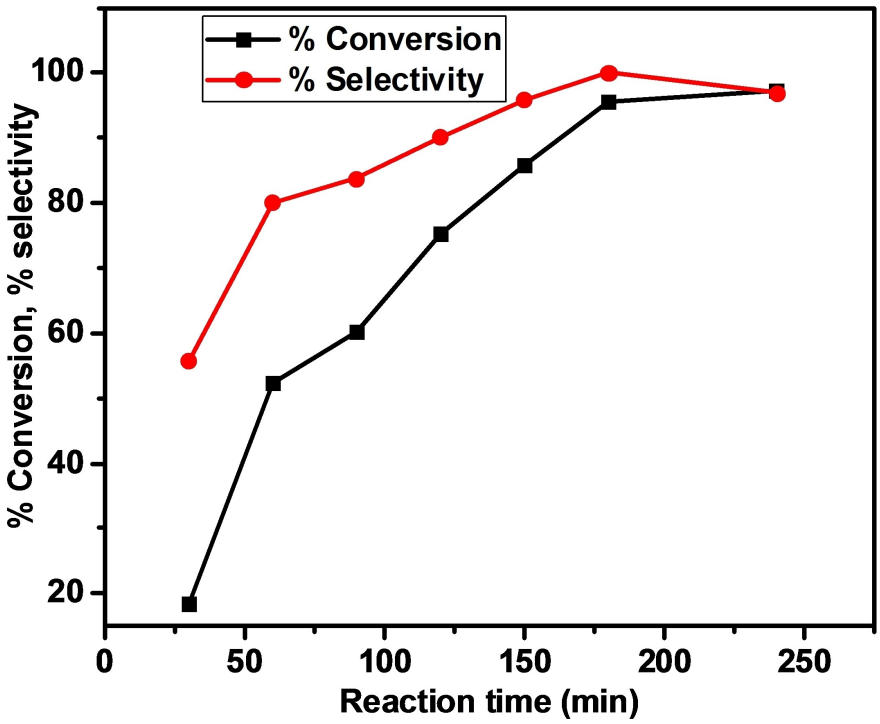

Figure 9. Effect of reaction time on the catalytic behaviour of 0.2 Fe_3O_4@g-C_3N_4 catalyst for the CTH of FF to FFA. Reaction conditions: 1 mmol FF, 10 mL ethanol, 20 mg catalyst, 373 K, reaction time from 0.5 h to 4 h, N_2 atmosphere.

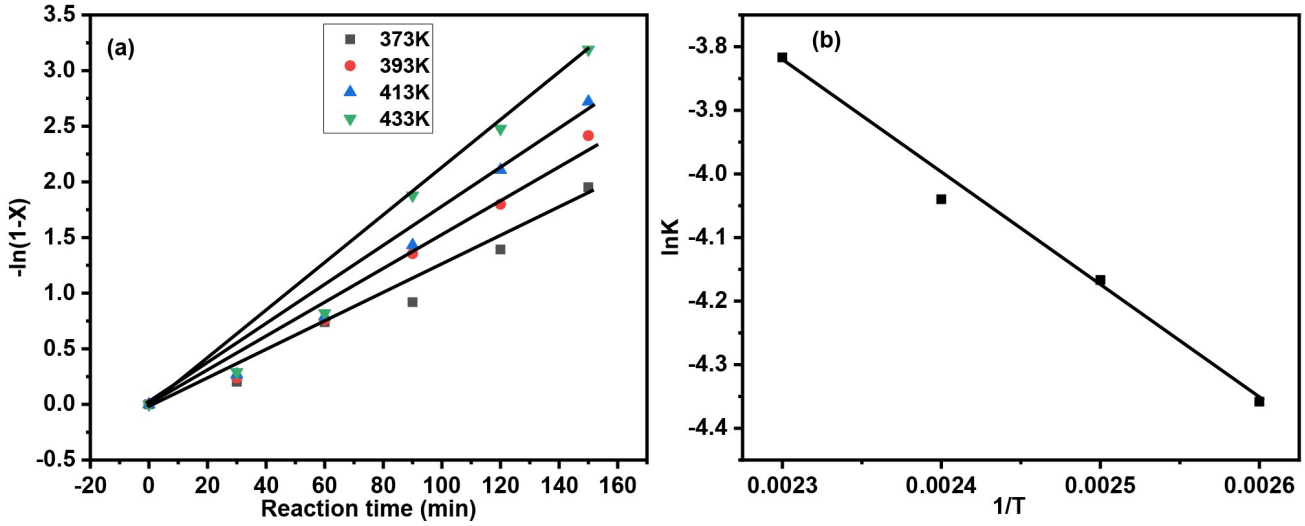

Figure 10. (a) Kinetic profiles of the FF to FFA conversion by the 0.2 Fe_3O_4@g-C_3N_4 (X, FF conversion) and (b) Arrhenius plot of formulation of FFA from FF.

Plausible reaction mechanism

Based on the described experimental results and previous literatures,[35,59] a possible mechanism for the transfer hydrogenation of FF was proposed (Scheme 2) in which CTH of furfural took place via MPV reduction over g-C_3N_4 supported magnetic ferrites species presuming the hydrogenation of the FF endures a six-membered ring coordination process. Firstly, ethanol molecule was adsorbed on the surface of Fe_3O_4@g-C_3N_4, followed by dissociation into corresponding alkoxide by interacting with the acid (Fe^{2+} or Fe^{3+}) and base sites (O^{2-}) of Fe_3O_4. Simultaneously, adsorption of C=O of furfural (FF) also took place on the catalytic surface which was activated by the acid-base sites. Further, transfer of hydrogen eventuated

Table 3. Comparative study of different reported catalysts with our catalyst.

Catalyst	FF conversion (%)	FFA yield (%)	Reaction conditions	Reference no.
CuO	86.5	41.8	Catalyst-90 mg, FF-1.2 mmol, methanol-15 mL, 513 K, 1.5 h, N_2(1 MPa)	[52]
Cu_2Al	> 99	54.7	Catalyst-90 mg, FF-1.2 mmol, methanol-15 mL, 513 K, 1.5 h, N_2(1 MPa)	[52]
γ- Fe_2O_3@HAP	96.2	91.7	Catalyst- 20 mg, FF-1 mmol, isopropanol-15 mL, 453 K, 3 h, N_2(1 MPa)	[16]
Al_7Zr_3	21.9	7.5	Catalyst- 40 mg, FF-2 mmol, isopropanol-10 mL, 393 K, 0.5 h, N_2(1 MPa)	[5]
Al_7Zr_3@Fe_3O_4	16.8	6.3	Catalyst- 40 mg, FF-2 mmol, isopropanol-10 mL, 393 K, 0.5 h, N_2(1 MPa)	[5]
Pd/C	30.2	0.8	Catalyst- 50 mg, FF-0.5 mmol, isopropanol-3 mL, 393 K, 6 h, N_2(1 MPa)	[13]
Ru/C	96.9	59.9	Catalyst- 50 mg, FF-0.5 mmol, isopropanol-3 mL, 393 K, 6 h, N_2(1 MPa)	[13]
Fe/C-800	34	25.4	Catalyst- 50 mg, FF-0.5 mmol, isopropanol-3 mL, 393 K, 6 h, N_2(1 MPa)	[13]
$Zr(OH)_4$	95.7	95.7	Catalyst- 75 mg, FF-1.2 mmol, isopropanol-15 mL, 423 K, 2.5 h, N_2(1 MPa)	[54]
2 wt% Pd/Fe_2O_3	100	34	Catalyst- 500 mg, FF-0.40 mol, isopropanol-40 mL, 453 K, 7.5 h, N_2(1 atm)	[17]
Co–Ru/C	98	98	Catalyst- 10 mg, FF-3.6 mmol, benzyl alcohol-10 mL, 423 K, 12 h, N_2(1 atm)	[55]
NiCoB	91.3	82	Catalyst- 20 mg, FF-0.06 mmol, ethanol-25 mL, 413 K, 2 h, H_2(3 MPa)	[25]
Cu/MgO	98	98	H_2/furfural ratio = 2.5, 453 K, 5 h	[14]
5%Pt/CN	60.9	>99	Catalyst- 50 mg, FF-0.4 mL, H_2O-10 mL, 373 K, 5 h, H_2(1 MPa)	[56]
$NiFe_2O_4$	95	95	Catalyst- 60 mg, FF-2 mmol, isopropanol-10 mL, 453 K, 4 h	[35]
20% Cu-MgO/Al_2O_3	100	89.3	Catalyst- 25 mg, FF-100 mg, isopropanol-5 mL, 483 K, 1 h, H_2 atmosphere	[57]
Ni–Fe (3/1) LDH	97	93	Catalyst- 20 mg, FF-100 mg, isopropanol-5 mL, 413 K, 5 h	[58]
Fe_3O_4/C	93.6	98.9	Catalyst- 50 mg, FF-2 mmol, isopropanol-10 mL, 2 MPa N_2, 473 K, 4 h	[59]
Fe_3O_4	97.5%	90.1	Catalyst- 100 mg, FF-0.6 mmol, isopropanol-20 mL, 433 K, 5 h	[60]
M–MOF-808	89.3%	79.1%	Mass ratio: Catalyst/Furfural/IPA: 0.1/1/25, 355 K, 2 h	[61]
0.2 Fe_3O_4@g-C_3N_4	95.6%	95.6%	Catalyst- 20 mg, FF-1 mmol, ethanol-10 mL, 373 K, 3 h, N_2 (1 atm.)	This work

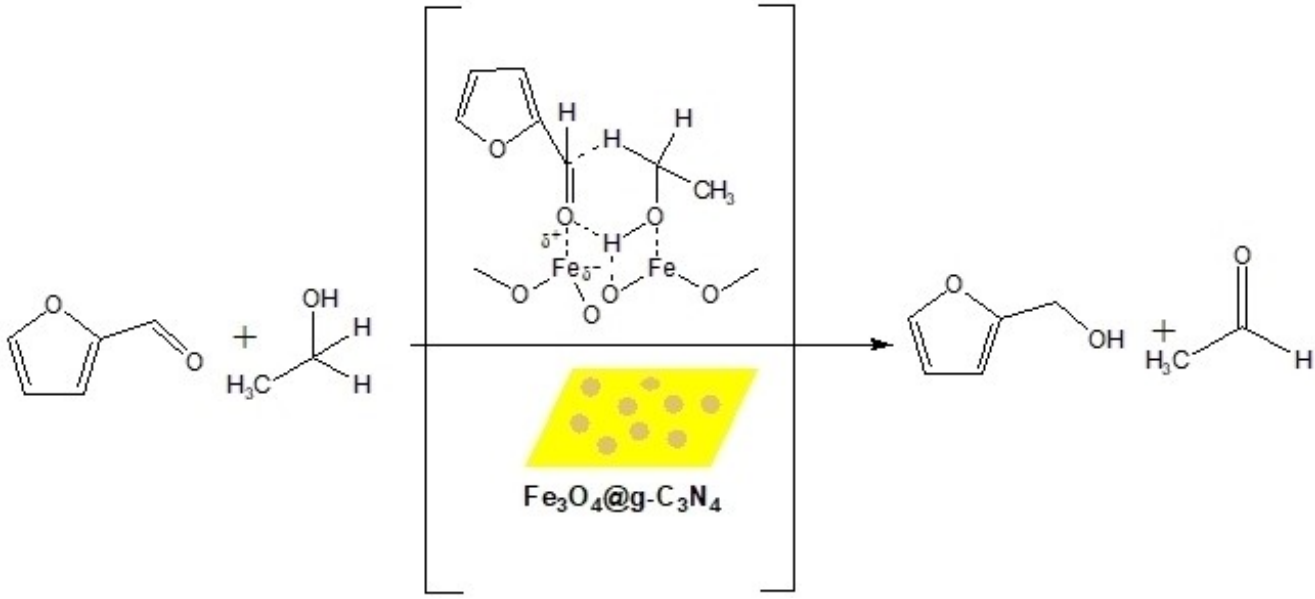

Scheme 2. Plausible reaction mechanism of transfer hydrogenation of furfural into furfuryl alcohol over magnetic Fe_3O_4@g-C_3N_4

between the dissociated alkoxide and the activated FF in a concerted manner involving a six-membered intermediate to form our desired product furfuryl alcohol (FFA) by releasing acetaldehyde. The 2D layer structure of nano compound would exhibit abundant reactive sites for adsorbing reactant molecules and this enhanced the adsorption of furfural. Also due to the superior electron mobility of 2D nano compound, CTH of furfural was much easier to perform to obtain the required product.

Catalyst Recyclability

Recyclability experiments of the 0.2 Fe_3O_4@g-C_3N_4 catalyst for the transfer hydrogenation of FF to FFA were conducted under optimised reaction conditions (Figure 11a). After each run, the catalyst Fe_3O_4@g-C_3N_4 was easily separated from the reaction mixture by using an external magnet. Soon after that the recovered catalyst was washed with water followed by ethanol and dried under vacuum at 60 °C. The catalyst was then precisely used in next catalytic run under identical reaction conditions. The furfural conversion and selectivity of the required product decrease marginally over five consecutive

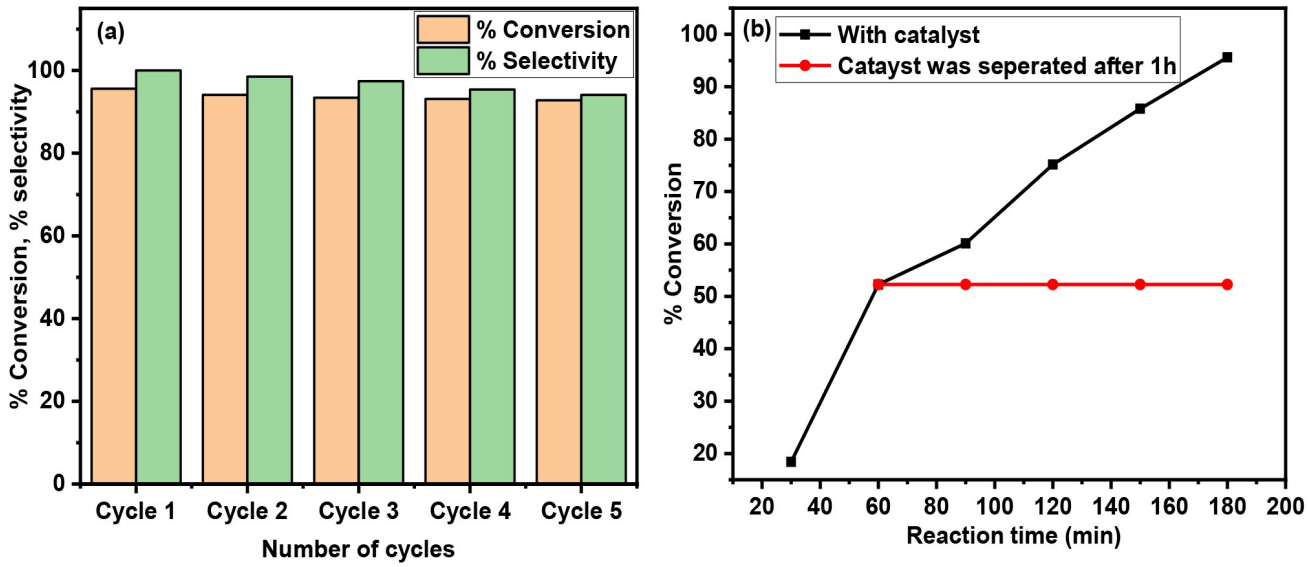

Figure 11. (a) Recyclability of 0.2 Fe_3O_4@g-C_3N_4 in the transfer hydrogenation of FF to FFA, (b) leaching experiment. Reaction conditions: 1 mmol FF, 10 mL ethanol, 20 mg catalyst, 373 K temperature, 3 h, N_2 atmosphere.

runs resulting in 92.8% conversion of furfural with 97.4% selectivity of furfuryl alcohol in the fifth run. Since, no notable changes were observed in all the catalytic cycles, so it can be narrated that the catalytic activity nearly remained persistent throughout the recyclability experiment.

The recycled catalyst is further characterised by using techniques PXRD, FTIR, XPS, SEM and TEM etc. and the constituents are enclosed in the electronic supplementary information (Figure S1, S2, S3, S4). The PXRD, FTIR, XPS analysis show no remarkable deviation of the signal peak positions. The morphology of the recovered catalyst is also found to be the same as evident from the SEM & TEM analysis.

A hot filtration test was also carried out to verify the heterogeneous nature of the catalyst during the reaction. For this, after one hour of the reaction, the solid catalyst was removed from the reaction mixture by an external magnet, and the reaction solution was subsequently allowed to react for another 2 h under the identical reaction conditions. It was observed that in absence of the catalyst no further conversion of FF (Figure 11b) was achieved; therefore, it may be assumed that no leaching of metal was occurred during the reaction signifying the heterogeneous nature of the catalyst.

Conclusions

A cost effective and benign magnetic ferrite Fe_3O_4@g-C_3N_4 catalyst was synthesized by a facile method, physiochemically characterised and demonstrated as efficient catalyst for the catalytic transfer hydrogenation of furfural into furfuryl alcohol using ethanol as both hydrogen donor and solvent. High furfural conversion of 95.6% with selectivity of furfuryl alcohol, 100% were obtained under optimised reaction conditions (3 h, 373 K temperature). Kinetic studies demonstrate that the CTH reaction was a pseudo first order reaction and the apparent activation energy, E_a of transfer hydrogenation was calculated to be 18 $kJmol^{-1}$. Leaching experiment confirms that the CTH reaction proceeded in a heterogeneous manner without leaching of metal and the catalyst can be reused under the optimum conditions without much alleviation in catalytic activity. The research thus spotlights a potential application like efficient catalytic transfer hydrogenation in the transformation of C=O bonds in various compounds like furfural to produce valuable fuels and chemicals using a cost-effective and easily separable g-C_3N_4 supported magnetic ferrite nanocatalyst in a very economical way.

Supporting Information

Experimental section, catalyst characterisation, XRD, FTIR, XPS data and SEM, TEM images of the recovered catalyst 0.2 Fe_3O_4@g-C_3N_4; atomic weight percentage of main metal element (Fe) present in the synthesised catalysts (from AAS data), ^{1}H NMR spectrum of product, GC graph of the reaction, GC-MS spectra of product.

Acknowledgements

The authors are thankful to the Director of CSIR-NEIST for allowing to publish the work. PB acknowledges DST, New Delhi for providing the INSPIRE Fellowship and LS is thankful to DST, New Delhi (Project No. GPP-0321) and in-house project OLP-2037 for financial support.

Conflict of Interest

The authors declare no conflict of interest.

Data Availability Statement

The data that support the findings of this study are available in the supplementary material of this article.

Keywords: furfural · furfuryl alcohol · g-C_3N_4 · magnetic ferrites · transfer hydrogenation

[1] J. C. Serano-Ruiz, R. Luque, A. Sepulveda-Escribano, *Chem. Soc. Rev.* **2011**, *40*, 5266–5281.
[2] A. Corma, S. Ibbora, A. Velty, *Chem. Rev.* **2007**, *107*, 2411–2502.
[3] K. L. Luska, P. Migowski, W. Leitner, *Green Chem.* **2015**, *17*, 3195–3206.
[4] R. D. Cortright, R. R. Davda, J. A. Dumesic, *Nature* **2002**, *418*, 964–967.
[5] J. He, Hu. Li, A. Riisager, S. Yang, *ChemCatChem.* **2018**, *10*, 430–438.
[6] H. Li, S. Yang, A. Riisager, A. Pandey, R. S. Sangwan, S. Saravanamurugan, R. Luque, *Green Chem.* **2016**, *18*, 5701–5735.
[7] R. J. van Putten, J. C. van der Waal, E. de Jong, C. B. Rasrendra, H. J. Heeres, J. G. de Vries, *Chem. Rev.* **2013**, *113*, 1499–1597.
[8] M. Audemar, C. Ciotonea, K. D. O. Vigier, S. Roger, A. Ungureanu, B. Dragoi, E. Dumitriu, F. Jérôme, *ChemSusChem.* **2015**, *8*, 1885–1891.
[9] C. P. Jimenez-Gomez, J. A. Cecilia, D. Duran-Martin, R. Moreno-Tost, J. Santamaria-Gonzalez, J. Merida-Robles, R. Mariscal, P. Maireless-Torres, *J. Catal.* **2016**, *336*, 107–115.
[10] Y. Yang, J. Ma, X. Jia, Z. Du, Y. Duan, J. Xu, *RSC Adv.* **2016**, *6*, 51221–51228.
[11] B. M. Reddy, G. K. Reddy, K. N. Rao, A. Khan, I. Ganesh, *J. Mol. Catal. A* **2007**, *265*, 276–282.
[12] B. M. Nakagawa, M. Tamura, Tomishige, K. Tomishige, *ACS Catal.* **2013**, *3*, 2655–2668.
[13] J. Li, J. Liu, H. Zhou, Y. Fu, *ChemSusChem.* **2016**, *9*, 1339–1347.
[14] B. M. Nagaraja, V. S. Kumar, V. Shasikala, A. H. Padmasri, B. Sreedhar, B. D. Raju, R. Rao, *Catal. Commun.* **2003**, *4*, 287–293.
[15] J. Wu, Y. Shen, C. Liu, H. Wang, C. Geng, Z. Zhang, *Catal. Commun.* **2005**, *6*, 633–637.
[16] F. Wang, Z. Zhang, *ACS Sustainable Chem. Eng.* **2017**, *5*, 942–947.
[17] D. Scholz, C. Aeliig, I. Hermans, *ChemSusChem* **2014**, *7*, 268–275.
[18] B. M. Nagaraja, A. H. Padmasri, B. D. Raju, K. S. Rama Rao, *J. Mol. Catal. A* **2007**, *265*, 90–97.
[19] W. E. Kaufmann, R. Adams, *J. Am. Chem. Soc.* **1923**, *45*, 3029–3044.
[20] Z. An, J. Li, *Green Chem.* **2022**, *24*, 1780–1808.
[21] C. Li, J. Li, L. Qin, P. Yang, D. G. Vlachos, *ACS Catal.* **2021**, *11*, 11336–11359.
[22] L. Cao, I. K. M. Yu, X. Xiong, D. C. W. Tsang, S. Zhang, J. H. Clark, C. Hu, Y. H. Ng, J. Shang, Y. S. Ok, *Environ. Res.* **2020**, *186*, 109547.
[23] L. Bui, H. Luo, W. R. Gunther, Y. Roman-leshkov, *Angew. Chem. Int. Ed.* **2013**, *52*, 8022–8025; *Angew. Chem.* **2013**, *125*, 8180–8183.
[24] M. Chia, J. A. Dumesic, *Chem. Commun.* **2011**, *47*, 12233–12235.
[25] J. He, H. Li, Y. Lu, Y. Liu, Z. Wu, D. Hu, S. Yang, *Appl. Catal. A* **2016**, *510*, 11–19.
[26] H. Li, J. He, A. Riisager, S. Saravanamurugan, B. Song, S. Yang, *ACS Catal.* **2016**, *6*, 7722–7727.
[27] P. Puthiaraj, K. Kim, W. S. Ahn, *Catal. Today* **2019**, *324*, 49–58.
[28] J. Du, J. Zhang, Y. Sun, W. Jia, Z. Si, H. Gao, X. Tang, X. Zeng, T. Lei, S. Liu, L. Lin, *J. Catal.* **2018**, *368*, 69–78.
[29] Z. Zhang, Z. Pei, H. Chen, K. Chen, Z. Hou, X. Lu, P. Ouyang, J. Fu, *Ind. Eng. Chem. Res.* **2018**, *57*, 4225–4230.
[30] M. J. Gilkey, P. Panagiotopoulou, A. V. Mironenko, G. R. Jenness, D. G. Vlachos, B. Xu, *ACS Catal.* **2015**, *5*, 3988–3994.
[31] M. Koehle, R. F. Lobo, *Catal. Sci. Technol.* **2016**, *6*, 3018–3026.
[32] M. M. Antunes, S. Lima, P. Neves, A. L. Magalhaes, E. Fazio, A. Fernandes, F. Neri, C. M. Silva, S. M. Rocha, M. F. Ribeiro, M. Pillinger, A. Urakawa, A. A. Valentine, *J. Catal.* **2015**, *329*, 522–537.
[33] T. Zeng, W. Chen, C. M. Cirtiu, A. Moores, G. Song, C. Li, *Green Chem.* **2010**, *12*, 570–573.
[34] B. Karami, S. J. Hoseini, K. Eskandari, A. Ghasemi, H. Nasrabadi, *Catal. Sci. Technol.* **2012**, *2*, 331–338.
[35] J. He, S. Yang, A. Riisager, *Catal. Sci. Technol.* **2018**, *8*, 790–797.
[36] J. Zhu, P. Xiao, H. Li, A. C. Carabneiro, *ACS Appl. Mater. Interfaces.* **2014**, *6*, 16449–16465.
[37] R. B. Nasir Baig, S. Verma, R. S. Varma, M. N. Nadagouda, *ACS Sustainable Chem. Eng.* **2016**, *4*, 1661–1664.
[38] M. J. Bojdys, J. O. Müller, Antonietti, A. Thomas, *Chem. Eur. J.* **2008**, *14*, 8177–8182.
[39] S. C. Yan, Z. S. Li, Z. G. Zou, *Langmuir.* **2009**, *25*, 10397–10401.
[40] Q. Wang, A. Chen, X. Wang, J. Zhang, J. Yang, X. Li, *J. Mol. Catal. A* **2016**, *420*, 159–166.
[41] J. Liu, T. Zhang, Z. Wang, G. Dawson, W. Chen, *J. Mater. Chem.* **2011**, *21*, 14398–14401.
[42] Y. Li, J. Zhang, Q. Wang, Y. Jin, D. Huang, Q. Cui, G. Zou, *J. Phys. Chem. B.* **2010**, *114*, 9429–9434.
[43] A. A. Said, M. M. M. Abd El-Wahab, M. Abd El-Aal, *Monatsh. Chem.* **2016**, *147*, 1507.
[44] J. Mao, T. Peng, X. Zhang, K. Li, L. Ye, L. Zan, *Catal. Sci. Technol.* **2013**, *3*, 1253–1260.
[45] D. Yang, T. Jiang, T. Wu, P. Zhang, H. Han, B. Han, *Catal. Sci. Technol.* **2016**, 6, 193–200.
[46] Y. Yao, Y. Cai, F. Lu, J. Qin, F. Wei, C. Xu, S. Wang, *Ind. Eng. Chem. Res.* **2014**, *53*, 17294–17302.
[47] W. Zhang, C. Kong, G. Lu, *Chem. Commun.* **2015**, *51*, 10158–10161.
[48] S. Bhuvaneswari, P. M. Pratheeksha, S. Anandan, D. Rangappa, R. Gopalan, T. N. Rao, *Phys. Chem. Chem. Phys.* **2014**, *16*, 5284–5294.
[49] L. Ge, *Mater. Lett.* **2011**, *65*, 2652–2654.
[50] Y. Zhai, Y. Dou, X. Liu, S. S. Park, C. .-S. Ha, D. Zhao, *Carbon* **2011**, *49*, 545–555.
[51] T. Nakagawa, S. Bjorge, R. W. Murray, *J. Am. Chem. Soc.* **2009**, *131*, 15578–15579.
[52] J. Zhang, J. Chen, *ACS Sustainable Chem. Eng.* **2017**, *5*, 5982–5993.
[53] H. Mao, C. Chen, X. P. Liao, B. Shi, *J. Mol. Catal. A* **2011**, *341*, 51–56.
[54] J. Zhang, K. Dong, W. Luo, H. Guan, *ACS Omega* **2018**, *3*, 6206–6216.
[55] Z. Gao, L. Yang, G. Fan, F. Li, *ChemCatChem* **2016**, *8*, 3769–3779.
[56] X. Chen, Li. Zhang, B. Zhang, X. Guo, X. Mu, *Sci. Rep.* **2016**, *6*, 1–13.
[57] H. Chen, H. Ruan, X. Lu, J. Fua, T. Langrish, X. Lu, *J. Mol. Catal.* **2018**, *445*, 94–101.
[58] T. Wang, A. Hu, H. Wang, Y. Xia, *J. Chin. Chem. Soc.* **2019**, *66*, 1610–1618.
[59] F. Li, S. Jiang, J. Huang, Y. Wang, S. Lu, C. Li, *New J. Chem.* **2020**, *44*, 478.
[60] M. Ma, P. Hou, P. Zhang, J. Cao, H. Liu, H. Yue, G. Tian, S. Feng, *Appl. Catal. A* **2020**, *602*, 117709.
[61] A. H. Valekar, M. Lee, J. W. Yoon, J. Kwak, D.-Y. Hong, K.-R. Oh, G. –Y Cha, Y.-U. Kwon, J. Jung, J.-S. Chang, Y. K. Hwang, *ACS Catal.* **2020**, *10*, 3720–3732.

Submitted: January 27, 2022
Accepted: April 29, 2022